

A COMPARISON OF THE OCTAVE-BAND DIRECTIONAL FILTER BANK AND GABOR FILTERS FOR TEXTURE CLASSIFICATION

Paul S. Hong

Center for Signal and
Image Processing
Georgia Institute of Technology
Atlanta, Georgia 30332
phong@ece.gatech.edu

Lance M. Kaplan

Center for Theoretical Studies of
Physical Systems
Clark Atlanta University
Atlanta, Georgia 30314
lkaplan@ieee.org

Mark J. T. Smith

School of Electrical and
Computer Engineering
Purdue University
West Lafayette, Indiana 47907
mjts@purdue.edu

ABSTRACT

This paper investigates the similarities between Gabor filters and the octave-band directional filter bank (OBDFB) with respect to texture classification. Both decompositions can discriminate angularly and radially in the 2-D frequency domain; however, the OBDFB has a computationally efficient implementation that makes it an attractive alternative to Gabor filters. An analysis of local energy features from Gabor filters and the OBDFB is presented showing similarities between their texture features. Texture classification experiments using both decompositions show comparable classification accuracy.

1. INTRODUCTION

The ability to classify the pixels of an image based on its surrounding pixels and textural cues plays a significant role in a number of image processing applications such as medical image processing and remote sensing. Typically, texture classification is divided into two subproblems: feature extraction and classification. This paper focuses on the feature extraction aspect of the texture classification problem. Filter banks and wavelets are able to generate features from images by decomposing them based on different frequency regions. By processing each subband and stacking the outputs, feature vectors can be formed. But with so many different decompositions, criteria must be defined to narrow the possibilities.

One particular approach to texture segmentation and analysis uses a polar-logarithmic Gabor filter bank where each Gabor filter represents a separate frequency channel thereby mimicking the human visual system (HVS). This approach is well-established for the texture segmentation problem [1], has been used in a wide variety of texture analysis systems, and has been analyzed with respect to a number of aspects already [2, 3].

One of the major reasons to use Gabor filters is because of its emulation of the cortex transform [4]. A side-by-side comparison is shown in Figure 1 where the analogous subband structures are evident. Additionally, Gabor filters are relatively easy to implement and conceptually simple.

Other decompositions have been used for the texture segmentation problem such as the directional filter bank (DFB) used by Rosiles in [5]. Although the DFB is unable to provide an octave-band decomposition, its ability to discriminate angularly allowed it to extract meaningful features in a maximally decimated and computationally efficient manner. The success of both the DFB and

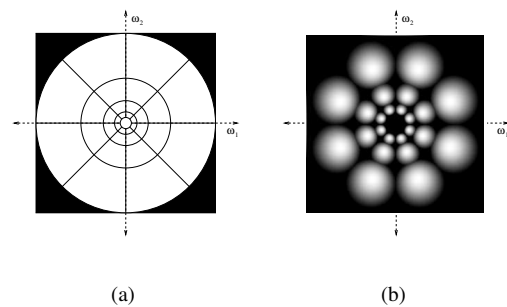


Fig. 1. (a) Channels of the cortex transform and (b) sample Gabor filters.

Gabor filters provides a strong case for multichannel approaches to texture classification, and in particular, results obtained using the DFB indicate that there is not necessarily a large trade-off between computational efficiency and high classification accuracy.

The octave-band directional filter bank (OBDFB) is able to capture similar directional and octave-band information as Gabor filters in a maximally decimated fashion in addition to having a computationally efficient implementation. The OBDFB also requires less memory than overcomplete decompositions. The purpose of this paper is to provide a comparison of the features extracted by the OBDFB and Gabor filter bank and to analyze actual texture classification results.

2. THE OCTAVE-BAND DIRECTIONAL FILTER BANK AND GABOR FILTERS

Gabor filters have been used very successfully for texture classification because of their ability to discriminate both angularly and radially in the frequency domain. Consequently, the filters are able to approximate different tilings of frequency space such as that of the cortex transform. A set of even-symmetric Gabor filters may be seen in Figure 1(b), and the impulse response (and associated frequency response) is characterized by the following Fourier

transform pair:

$$h(x, y) = \frac{1}{2\pi\sigma_x\sigma_y} \exp\left\{-\frac{1}{2}\left[\frac{x^2}{\sigma_x^2} + \frac{y^2}{\sigma_y^2}\right]\right\} \cos(2\pi u_0 x),$$

$$H(u, v) = A \left(\exp\left\{-\frac{1}{2}\left[\frac{(u-u_0)^2}{\sigma_u^2} + \frac{v^2}{\sigma_v^2}\right]\right\} + \exp\left\{-\frac{1}{2}\left[\frac{(u+u_0)^2}{\sigma_u^2} + \frac{v^2}{\sigma_v^2}\right]\right\} \right),$$

where u_0 is the frequency of a sinusoidal plane wave along the x -axis; σ_x and σ_y are the space constants of the Gaussian envelope along the x and y axes, respectively; $\sigma_u = 1/2\pi\sigma_x$ and $\sigma_v = 1/2\pi\sigma_y$; and $A = 2\pi\sigma_x\sigma_y$ [1]. Filters with arbitrary orientations are obtained by a rotation of the $x - y$ coordinate system. The Fourier representation is clearly a pair of Gaussians oriented in a particular direction with some radial center frequency. The directional partitioning in addition to the octave-band structure is apparent in the figure even though the filters themselves are far from ideal with respect to well defined passbands (i.e., passband overlap).

The OBDFB was originally proposed in [6]. It is a maximally decimated 2-D transform that can partition the frequency plane both angularly and radially. An instance of the OBDFB similar to the decompositions shown in Figure 1 may be seen in Figure 2 where there are 4 directions and 3 octave bands. Although the OBDFB does not have a uniform center radial frequency for the octave bands (because of square tilings vs. the circular tilings of the Gabor filters), the overall structure is similar and approximates both the Gabor filter bank and the cortex transform quite well.

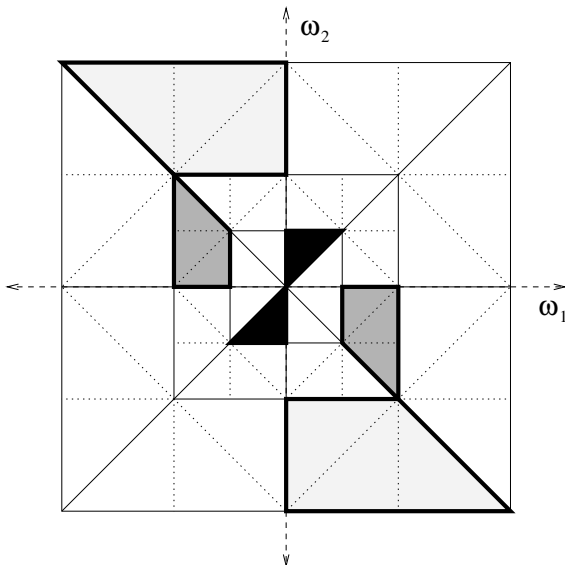


Fig. 2. A 4-direction, 3-octave OBDFB. Certain regions are shaded for emphasis of subband combinations.

Advantages of the OBDFB system include the use of linear-phase filters, perfect reconstruction, and control of both angular and radial frequency resolution. However, the greatest advantage over Gabor filters comes from the computational efficiency. Be-

cause the OBDFB is maximally decimated, computations are reduced at each stage in addition to saving memory. Also, the OBDFB uses a polyphase form for its 2-band filter banks that, in turn, allows for separable filtering. For example, a set of Gabor filters might be implemented for N_d directions and N_o octave bands. Although more efficient implementations exist for Gabor filters, a comparison using the simplest case is still effective. If the filters are of size $N \times N$, then there are $N_d \times N_o \times N \times N$ multiplies per pixel. For a comparable OBDFB, the number of multiplies for the directional decomposition is $2 \times N \times \log_2 N_d$ per pixel, and the number for the octave-decomposition is $2 \times 2 \times N \times \frac{1 - (\frac{1}{4})^{N_o - 1}}{1 - \frac{1}{4}}$ per pixel. Computational savings become significant for larger images with a large number of subbands; for example, a 256×256 image decomposed using 4 directions and 3 octave bands and length 12 filters yields 113 million multiplies for the Gabor filter bank but only 7.1 million multiplies using the OBDFB, a $\frac{1}{16}$ th of the multiplies needed for the Gabor filters. Obviously the savings increase dramatically with filter length N . Additionally, the use of symmetric filters can halve the number of computations for the OBDFB.

3. SYSTEM OVERVIEW

There are many different configurations used for texture classification using filtering techniques. For this system, complexity was a factor in the choice of components, but the underlying units are typically the same from system to system. After the input image is decomposed, local energy estimates from each subband are used to create feature vectors which are then classified. Because the purpose of this research is to compare Gabor filters with the OBDFB, the system was made as modular as possible such that switching between the decompositions was easily accomplished. As for Gabor filter bank parameters, the σ values were chosen to obtain even coverage of the spectrum given the number of directions and octave bands. Ultimately, the overall texture classification system from [7] was used with minor adjustments.

Energy estimation was performed after a zero-order hold interpolation of the OBDFB subbands to the size of the original image so that the smoothing filter would remain consistent between the two transforms. For energy estimation, the square-magnitude of the subband coefficients is smoothed in both the horizontal and vertical directions by using a Gaussian smoothing filter of the form

$$h_G[n] = \frac{1}{\sqrt{2\pi}\sigma_s} \exp\left(-\frac{1}{2} \frac{n^2}{\sigma_s^2}\right), \quad (1)$$

where $\sigma_s = 8$. The log is then taken of the smoothed data.

In order to approximate the octave-band subbands of the Gabor filters, a modification was made to the OBDFB system. Typically at each octave-band split, 4 subbands are generated, the radially low frequency subband and three other radially high frequency subbands. Because the feature vector is generated by a local energy estimation, the energy of the three radial high frequency subbands is summed together to form a single dimension of the feature vector.

For both decompositions, the low frequency region was removed separately with a cut-off frequency of $\frac{\pi}{16}$ and processed as its own dimension within the feature vector. This was necessary for both transforms as the Gabor filter bank implementation excludes the low frequency region and the OBDFB tends to propagate the DC region into a single directional band.

For classification, type 1 learning vector quantization (LVQ) used by Randen [7] was employed. If m_i represents the codebook vectors, then some vector x is declared to be in the same class C as the nearest m_i which will be denoted as m_n . The training process is described for input $x[k]$ (where k denotes time) as

$$m_n[k+1] = \begin{cases} m_n[k] + \alpha[k](x[k] - m_n[k]), & \text{if } x, m_n \in C, \\ m_n[k] - \alpha[k](x[k] - m_n[k]), & \text{otherwise,} \end{cases}$$

where $0 < \alpha[k] < 1$ and $\alpha[k]$ may be constant or decrease monotonically with time, and the m_i for $i \neq n$ do not change. The number of codebook vectors used was 800, and the training data was kept strictly separate from the test data.

After codebook generation, each of the test vectors was assigned to a class according to comparison with the codebook vectors, and texture maps were generated. Another reason smoothing is applied after resizing the subbands for the OBDFB is to allow use of the same ground truth (i.e., not resizing the ground truth to accommodate even the largest decimated subband).

4. RESULTS

One impetus for using the OBDFB as an alternative to Gabor filters is that they are able to approximate the same frequency partitions. Unfortunately, direct comparison of transform subbands is not particularly enlightening because of the decimation-induced aliasing that occurs in the case of the OBDFB; however, feature comparison is reasonable because of the processing methods. In this case, because energy is taken, it is reasonable to sum energy components in the three subbands of the OBDFB that typically make up the higher radial frequency octaves. Additionally, because a smoothing filter is used to blur fine structures to a certain extent, it is possible to see similar structures. Test collages of Brodatz textures may be seen in Figure 3 taken from [7].

Selected texture feature components are shown in Figure 4. Although there are obvious differences, the overall structures appear consistent. Because of the maximal decimation and its associated interpolation, the OBDFB features are not always as well defined as the Gabor equivalents; however, a closer inspection yields promising results.

Texture classification results for different Gabor filter bank and OBDFB parameters are given in Table 1. The number of subbands generated must be restricted so that the resolution of the OBDFB subbands does not become too low. The OBDFB performs comparably with the Gabor filters as noted more by the output maps (a sample of which is shown in Figure 5) than the table of results. The scores from Table 1 are fairly consistent with those from [7] (although the systems use different smoothing filters).

A similar OBDFB texture classification system has also been used to augment spectral features in hyperspectral data classification [8]. The texture augmentation was able to increase classification accuracy in addition to decreasing the amount of misclassification in homogeneous regions.

5. CONCLUSION

The OBDFB provides a computationally efficient alternative to using Gabor filters for texture classification. Although the resulting features are not identical, the most important structures are retained and classification results are comparable, especially considering the significant reduction in computations.

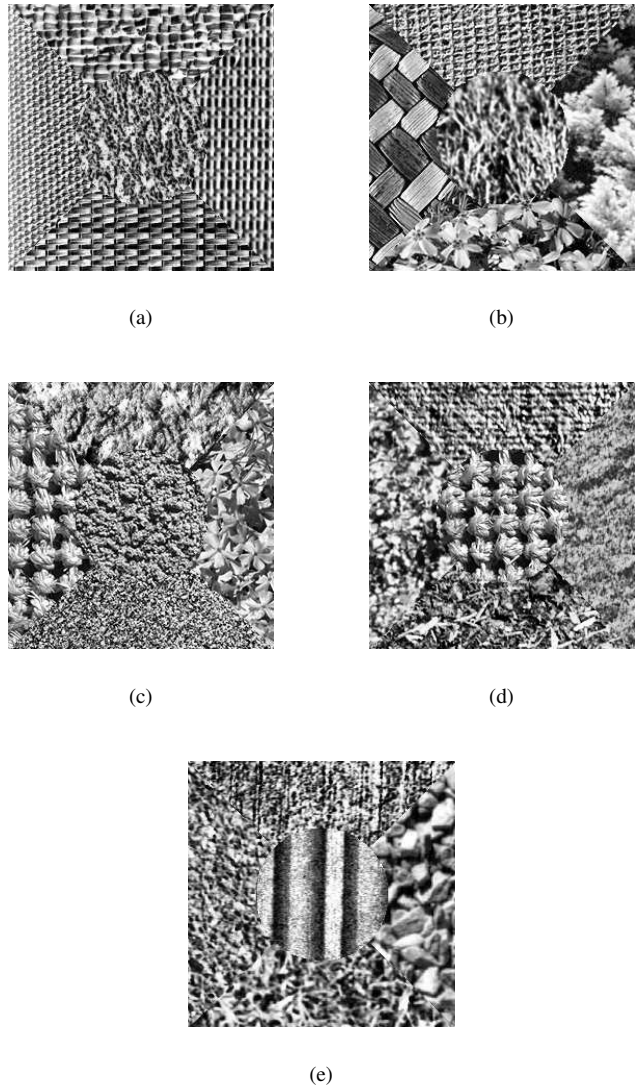


Fig. 3. (a) 5-texture Brodatz test images from [7] used for the experiments whose results are presented in Table 1.

6. REFERENCES

- [1] A. K. Jain and F. Farrokhnia, "Unsupervised texture segmentation using Gabor filters," *Pattern Recognition*, vol. 24, no. 12, pp. 1167–1186, 1991.
- [2] D. A. Clausi and M. E. Jernigan, "Designing Gabor filters for optimal texture separability," *Pattern Recognition*, vol. 33, pp. 1835–1849, 2000.
- [3] S. E. Grigorescu, N. Petkov, and P. Kruizinga, "Comparison of texture features based on Gabor filters," *IEEE Trans. on Image Processing*, vol. 11, no. 10, pp. 1160–1167, Oct. 2002.
- [4] A. B. Watson, "The cortex transform: Rapid computation of simulated neural images," *Computer Vision, Graphics, Image Processing*, vol. 39, no. 3, pp. 311–327, 1987.
- [5] R.-G. Rosiles and M. J. T. Smith, "Texture segmentation with

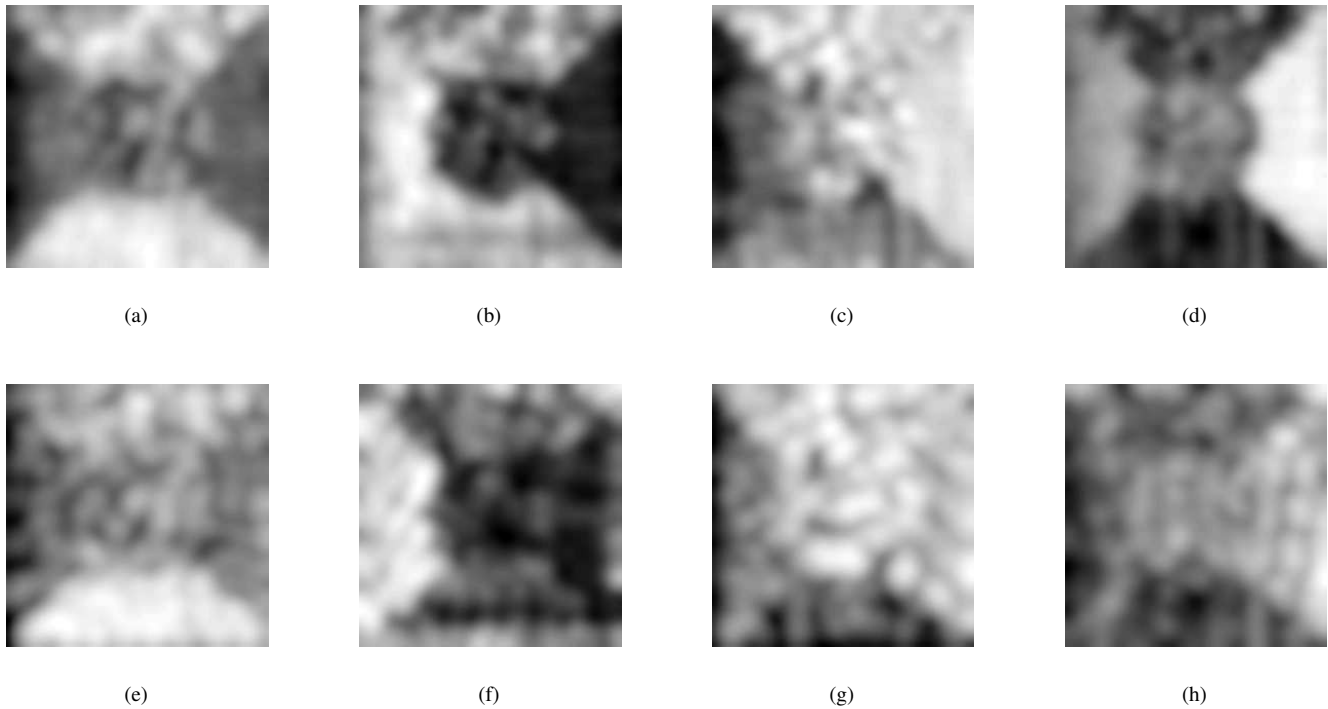


Fig. 4. Examples of features extracted from the image shown in Figure 3(a) from analogous subbands from a Gabor filter bank ((a) – (d)) and the OBDFB ((e) – (h)). The decomposition has 4 angular components and 3 octave bands. In each case, the feature values were shifted and scaled to fill the dynamic range for visualization.

Decomp.	Test Image					mean
	3(a)	3(b)	3(c)	3(d)	3(e)	
Gabor 4,2	10.1	24.1	27.1	24.1	11.1	19.3
Gabor 4,3	6.2	21.3	27.8	24.2	10.0	17.9
Gabor 4,4	6.8	16.7	30.4	23.6	12.5	18.0
Gabor 8,2	7.8	19.0	27.4	25.3	11.0	18.1
Gabor 8,3	6.6	17.4	27.8	23.7	10.5	17.2
OBDFB 4,2	16.2	30.9	42.3	39.2	27.3	31.2
OBDFB 4,3	11.8	29.0	40.8	38.0	24.5	28.8
OBDFB 4,4	13.2	27.0	45.7	43.6	29.4	31.8
OBDFB 8,2	12.0	22.3	37.9	41.2	25.8	27.8
OBDFB 8,3	9.9	26.9	38.2	37.8	24.7	27.5

Table 1. Average texture segmentation results (% inaccurate). The decompositions are labeled first by type, then by number of directions and number of octave bands, respectively.

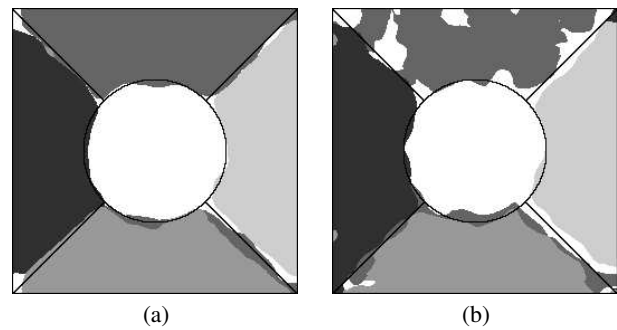


Fig. 5. (a) Gabor filter bank output and (b) OBDFB output each decomposition having 4 directions and 3 octave bands.

a biorthogonal directional decomposition,” in *World Multi-conference on Systemics and Informatics*, July 2000.

- [6] P. S. Hong and M. J. T. Smith, “An octave-band family of non-redundant directional filter banks,” in *IEEE Proceedings: ICASSP*, 2002, pp. 1165–1168.
- [7] T. Randen and J. Håkon Husøy, “Filtering for texture classification: A comparative study,” *IEEE Transactions on Pattern Analysis and Machine Intelligence*, vol. 21, no. 4, pp. 291–310, Apr. 1999.
- [8] P. S. Hong, L. M. Kaplan, and M. J. T. Smith, “Hyperspectral

image segmentation using filter banks for texture augmentation,” in *IEEE Workshop on Advances in Techniques for Analysis of Remotely Sensed Data*, 2003.